Cell, Vol. 101, 485–498, May 26, 2000, Copyright ©2000 by Cell Press

ETS Gene *Er81* Controls the Formation of Functional Connections between Group Ia Sensory Afferents and Motor Neurons

Silvia Arber,*§ David R. Ladle,† Jonathan H. Lin,* Eric Frank,† and Thomas M. Jessell*‡
*Howard Hughes Medical Institute
Department of Biochemistry and Molecular Biophysics
Center for Neurobiology and Behavior
Columbia University
New York, New York 10032
†Department of Neurobiology
University of Pittsburgh
Pittsburgh, Pennsylvania 15261

Summary

The connections formed between sensory and motor neurons (MNs) play a critical role in the control of motor behavior. During development, the axons of proprioceptive sensory neurons project into the spinal cord and form both direct and indirect connections with MNs. Two ETS transcription factors, ER81 and PEA3, are expressed by developing proprioceptive neurons and MNs, raising the possibility that these genes are involved in the formation of sensory-motor connections. *Er81* mutant mice exhibit a severe motor discoordination, yet the specification of MNs and induction of muscle spindles occurs normally. The motor defect in *Er81* mutants results from a failure of group Ia proprioceptive afferents to form a discrete termination zone in the ventral spinal cord. As a consequence there is a dramatic reduction in the formation of direct connections between proprioceptive afferents and MNs. ER81 therefore controls a late step in the establishment of functional sensory-motor circuitry in the developing spinal cord.

Introduction

The precision with which neuronal circuits are assembled during development has a fundamental role in defining the behavioral repertoire of the mature organism. The formation of neuronal connections depends on a series of developmental steps that include the extension of axons toward distant targets (Tessier-Lavigne and Goodman, 1996), the selection of specific laminar termination zones within target regions (Sanes and Yamagata, 1999) and the formation of selective synapses (Frank et al., 1988). There is increasing evidence that many aspects of neuronal development are directed by the cell type–specific expression of transcription factors (Bang and Goulding, 1996; Cepko, 1999). However, most transcription factors that have been implicated in neural differentiation control early developmental processes: the specification of regional neural pattern (Lumsden and Krumlauf, 1996) and neuronal identity (Tanabe and Jessell, 1996) and the selection of early axonal trajectories (Landgraf et al., 1999; Thor et al., 1999). It remains unclear whether and how cell-specific transcription factors control later developmental steps that more directly influence neuronal connectivity and function.

Within the vertebrate central nervous system (CNS), the simplest and best understood neuronal circuit is that controlling a stereotyped sensory-motor behavior, the spinal monosynaptic stretch reflex circuit (Eccles et al., 1957; Brown, 1981). In this circuit, connections are formed between two main classes of neurons, muscle sensory (proprioceptive) neurons and spinal motor neurons (MNs). The axons of proprioceptive neurons enter the spinal cord during embryonic development and form either direct or indirect connections with MNs. This distinction in connectivity reflects the existence of two major classes of proprioceptive neurons, distinguishable by their association with specialized peripheral transduction cells and by their pattern of axonal projections in the spinal cord (Brown, 1981; Zelena, 1994).

One class of proprioceptive neurons, group Ia afferents, innervates muscle spindles in the periphery. Centrally, group Ia afferents form two major termination zones, one in the intermediate spinal cord where synapses are made with interneurons and one in the ventral spinal cord where direct connections are made with MNs (Brown, 1981). A second class, group Ib afferents, forms peripheral associations with Golgi tendon organs (GTOs) and projects axons centrally only to the intermediate spinal cord, where synaptic contacts are made with interneurons but not with MNs (Brown, 1981). At a finer level of specificity, muscle spindle afferents form preferential connections with pools of MNs that innervate the same muscle group (Eccles et al., 1957; Frank et al., 1988). The selectivity of connections formed between proprioceptive afferents and MNs is thought to have its basis in the selection of distinct afferent termination zones in the spinal cord and the recognition of specific neuronal targets (see Chen and Frank, 1999), but functional insight into the molecules that control the development of this circuit has not been obtained.

In avian embryos, developing proprioceptive neurons and MNs are linked by the expression of ER81 and PEA3, two closely related members of the ETS class of transcription factors (Lin et al., 1998). Initially, ER81 and PEA3 are coexpressed by all proprioceptive neurons, but the expression of these two proteins soon segregates into distinct neuronal subsets. At the time that direct sensory-motor connections are formed, individual pools of MNs that express ER81 or PEA3 are innervated preferentially by proprioceptive afferents that express the same ETS protein (Lin et al., 1998). ETS proteins control cell differentiation in many nonneural systems (Wasylyk et al., 1998), raising the possibility that the expression of ER81 and PEA3 contributes to the formation of selective connections between proprioceptive afferents and MNs in the developing spinal cord (Lin et al., 1998).

We have analyzed the development of sensory-motor

‡To whom correspondence should be addressed (e-mail: tmj1@columbia.edu).
§Present address: Department of Cell Biology, University of Basel, Basel CH-4056, Switzerland.

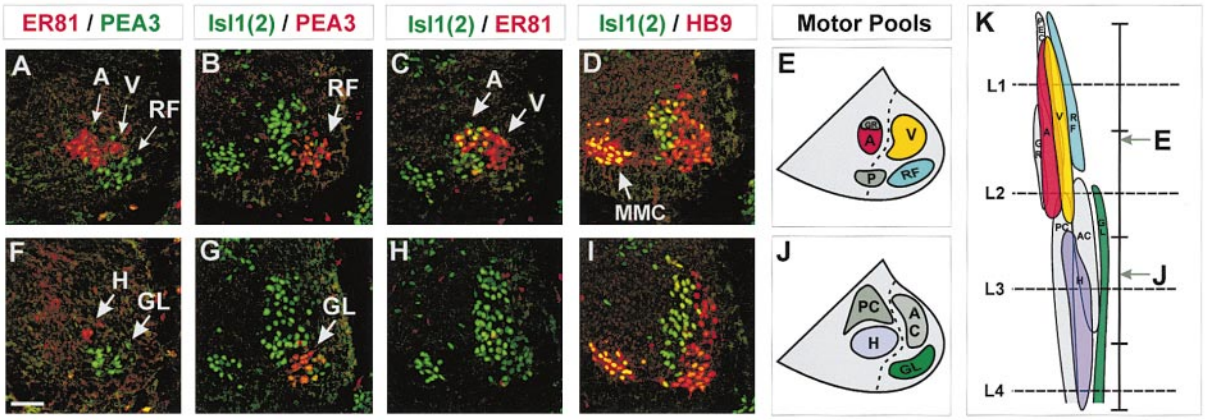

Figure 1. Expression of ER81 and PEA3 in Developing MNs

(A–D, F–I) Expression of ER81 and PEA3 in motor pools of the ventral quadrant of lumbar spinal cord of E13.5 mouse embryos at L2 (A–D) and L3 (F–I) (lateral is to the right). Motor pools are indicated by arrows: A, adductor; V, vasti; RF, rectus femoris; H, hamstring; GL, gluteus. (A and F) Expression of ER81 (red) and PEA3 (green). At L2, ER81 is expressed in A MNs (LMCm; also see Figures 1C and 5) and in V MNs (LMCl; also see Figure 1C), whereas PEA3 is expressed in RF MNs. At L3, ER81 is expressed by a subset of H MNs and PEA3 is expressed by GL MNs.

(B and G) Lateral PEA3$^+$ RF MNs (B) and GL MNs (G) do not coexpress Isl1 (LMCl).

(C and H) At L2 A MNs coexpress Isl1 (LMCm) and V MNs do not express Isl1 (LMCl). At L3, the majority of Isl1$^+$/ER81$^-$/PEA3$^-$ MNs correspond to PC and H MNs.

(D and I) The level of HB9 expression is higher in LMCl than in LMCm. MMC MNs (arrow) coexpress high levels of HB9 and Isl1 (appearing yellow).

(E and J) Motor pool map at L2 (E) and L3 (J) (modified from McHanwell and Biscoe, 1981). Motor pools that express either ER81 or PEA3 are shown in color. A: adductor, red (ER81$^+$/Isl1$^+$, LMCm); V: vasti, yellow (ER81$^+$/Isl1$^-$, LMCl); RF: rectus femoris, turquoise (PEA3$^+$/ Isl1$^-$); GL: gluteus, green (PEA3$^+$/Isl1$^-$); H: hamstring muscles (blue) comprise several motor pools only a subset of which express ER81 or PEA3. P, pectineus; PC, posterior cruz; AC: anterior cruz. Dashed lines represent border between LMCm (left) and LMCl (right).

(K) Reconstructed motor pools in a horizontal section of lumbar spinal cord. Horizontal lines marked as L1–L4 represent the posterior end of each segment. Gray arrows to the right (E and J) indicate level corresponding to the transverse sections in (A–E) and (F–J).

Scale bar = 30 μm.

connections in mice lacking *Er81* function. *Er81* mutant mice develop a severe defect in motor coordination, but this behavorial phenotype is not associated with a disruption in the generation of proprioceptive neurons or MNs, nor in the initial pattern of axonal projections of these neurons. Rather, in *Er81* mutant mice, group Ia muscle spindle afferents fail to form their characteristic termination zone in the ventral spinal cord. As a consequence, direct connections between proprioceptive afferents and MNs are dramatically reduced and functional motor output is lost. These results provide genetic evidence that a late step in the assembly of sensory-motor circuitry in the mammalian CNS is controlled by an ETS class transcription factor.

Results

Expression of ER81 and PEA3 by MNs and Proprioceptive Neurons

We first examined the profile of expression of ER81 and PEA3 by MNs during mouse embryonic and postnatal development. At limb levels of the spinal cord ER81 and PEA3 were expressed by nonoverlapping subsets of MNs within the lateral motor column (LMC), but were excluded from neurons in the median motor column (MMC) (Figures 1A–1J). PEA3 expression was first detected at ~E11.0 and ER81 expression at E12.0, and the expression of both proteins persisted in subsets of LMC neurons until at least P10 (data not shown).

To determine the identity of the hindlimb LMC neurons that expressed ER81 and PEA3, we compared their position with that of MN pools (McHanwell and Biscoe, 1981; C. Lance-Jones, Soc. Neurosci. abstract *10*, 639, 1984). We also injected HRP into selected hindlimb muscles and examined the ETS protein profile of retrogradely labeled MNs. ER81 appears to be expressed in the vasti, adductor, and a subset of hamstring MNs (Figures 1A–1K; data not shown), whereas PEA3 expression maps to the rectus femoris, gluteus and a separate set of hamstring MNs (Figures 1A–1K; data not shown). At forelimb levels, PEA3 was expressed by pectoralis MNs but few LMC neurons expressed ER81 (data not shown). Thus in mouse as in chick, the expression of ER81 and PEA3 defines distinct MN pools. Moreover, the MN pools that express ER81 or PEA3 in the mouse appear to supply the functional homologs of chick muscles innervated by ER81$^+$ and PEA3$^+$ LMC neurons (Lance-Jones, 1979).

We next examined whether ER81 and PEA3 are also expressed by developing DRG neurons. We focused on the L4 and L5 DRG, but similar findings were obtained at other segmental levels (data not shown). Expression of PEA3 was first detected at E12.5, and ER81 at E13.0 (Figures 2A–2C; data not shown). Individual DRG neurons, however, showed varied levels of ER81 expression (arrows in Figure 2B). Between E13.0 to E14.0, ~20% of all DRG neurons, defined by Isl1 expression, expressed ER81 and ~15% expressed PEA3 (Figure 2B; data not

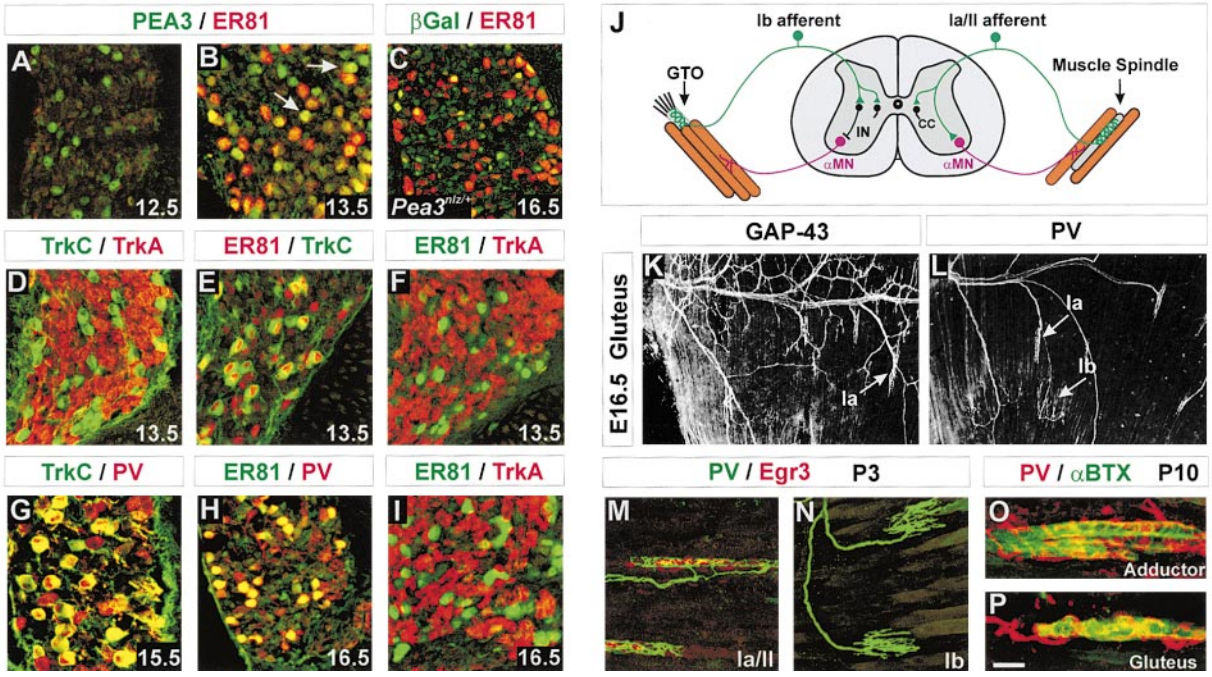

Figure 2. ER81 Expression in Developing DRG Neurons

(A–I) Expression of ER81, PEA3, and markers of cutaneous or proprioceptive neurons in developing L4 and L5 DRG.

(A–C) Expression of ER81 (red) and PEA3 (green) in wild-type embryos (A and B) and ER81 (red) and β-gal (green) in *Pea3*$^{nlslacZ/+}$ embryos (C). The level of ER81 and PEA3 varied between individual neurons (white arrows in (B) indicate neurons expressing a low level of ER81 and high level of PEA3). At E16.5, *Pea3* expression was assessed in a mouse strain carrying a targeted *nlslacZ* insertion into the *Pea3* locus. LacZ expression in this line closely recapitulates endogenous PEA3 expression (S. A. and T. M. J., unpublished). The incidence of coexpression of ER81 and *Pea3* is ~15% of all ETS$^+$ neurons. At E16.5 ~20% of PV$^+$ neurons expressed lacZ, and ~10% of TrkA$^+$ neurons expressed lacZ (data not shown). Thus, PEA3 appears to be expressed by a subset of proprioceptive neurons and also by some cutaneous neurons.

(D) Expression of TrkC (green) and TrkA (red) defines distinct neuronal populations in E13.5 DRG.

(E) ER81 (red) is coexpressed in TrkC$^+$ (green) neurons. ER81 is also expressed by some TrkC$^-$ cells (~30% of ER81$^+$ cells).

(F) ER81 (red) expression is excluded from TrkA$^+$ (red) neurons at E13.5.

(G) Coincidence of expression of TrkC (green) and PV (red) in E15.5 DRG.

(H) At E16.5, the majority (>95%) of PV$^+$ (red) cells coexpress ER81 (green).

(I) At E16.5, ER81 (red) is excluded from TrkA$^+$ (red) neurons.

(J) Peripheral and central projections of group Ia/II and group Ib afferents (green). Left: group Ib muscle afferent receive sensory input from GTOs and project to the intermediate spinal cord, making indirect connections with α-MNs (purple) through interneurons (IN). Right: group Ia/II muscle afferents innervate muscle spindles in the periphery (gray). The central branches of group Ia/II afferents make direct connections with α-MNs (purple) and also indirect connections. Both group Ia/II and group Ib afferents have a termination zone in the intermediate spinal cord in the region of Clarke's column (CC) neurons.

(K and L) Innervation of the gluteus muscle at E16.5 visualized in whole mount by GAP-43 (K) or PV (L) expression. GAP-43 labels motor and sensory axons whereas PV selectively labels proprioceptive axons. PV$^+$ fibers innervating muscle spindles are indicated by white arrows (Ia). Regions of afferent innervation of GTOs (indicated by white arrows; Ib) are found preferentially at the site of muscle insertion. Proprioceptive nerve branches terminate at both muscle spindles and GTOs. Motor axons terminate in the central region of the muscle (fine GAP-43$^+$ branches in [K]).

(M and N) PV$^+$ (green) proprioceptive afferents innervate Egr3$^+$ (red) muscle spindles (M) and Egr3$^-$ nascent GTOs (N) in P3 gluteus muscle. The group Ib ending shows a characteristic flame-shaped ending (N) whereas the group Ia/II ending associated with muscle spindles has an annulospiral form (M).

(O and P) Muscle spindles in P10 adductor (O) and gluteus (P) muscles express AChR (α-bungarotoxin$^+$; α-BTX; green) and are innervated by PV$^+$ proprioceptive afferents.

Scale bars: (A, C, D–F, H, O, and P) = 20 μm; (B, G, and I) = 15 μm; (K and L) = 100 μm; (M and N) = 35 μm.

shown). At this stage, >90% of ER81$^+$ cells coexpressed PEA3 (Figure 2B; data not shown), but by E15.5 this number had decreased to ~10% (Figure 2C; data not shown).

To determine which classes of DRG neurons express these ETS proteins, we examined the coexpression of ER81 and PEA3 with TrkC and parvalbumin (PV), markers of proprioceptive neurons and with TrkA, a marker of small diameter cutaneous neurons (Figures 2D–2I; Mu et al., 1993; Honda, 1995). At E13.5, all TrkC$^+$ neurons coexpressed ER81, ~30% of ER81$^+$ neurons lacked TrkC expression (Figure 2E), but no TrkA$^+$ neurons expressed ER81 (Figure 2F). From E16.0, TrkC expression could not reliably be detected with available antibodies, but PV expression marked all proprioceptive neurons. PV was expressed by muscle spindle (group Ia and group II) and GTO (group Ib) afferents and was excluded from cutaneous neurons (Figures 2G, 2H, 2J–2P). From E16.5 to P10, expression of ER81 was detected in virtually all PV$^+$ proprioceptive neurons (Figure 2H; data not

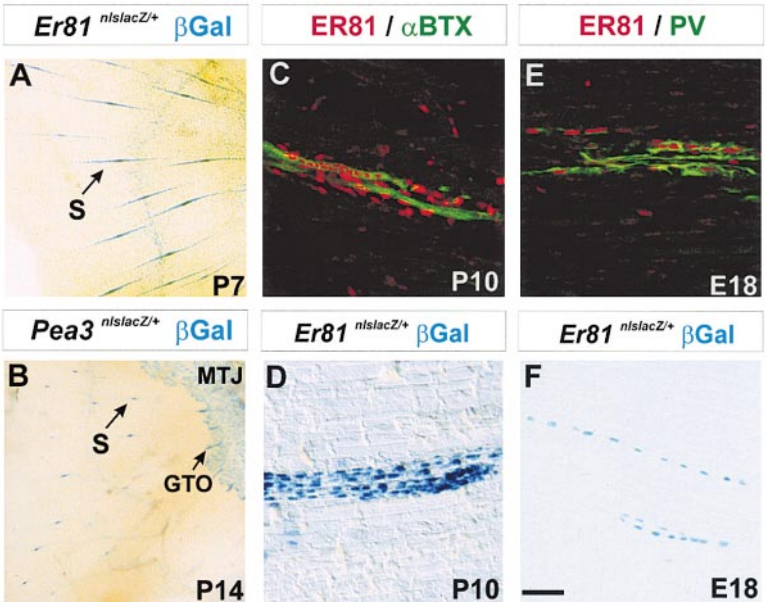

Figure 3. ER81 and PEA3 Expression in Developing Muscle Spindles

(A) Low magnification view of the gluteus muscle of a P7 *Er81*$^{nlslacZ/+}$ embryo processed for β-gal activity. The arrow indicates a muscle spindle (S). A low level of β-gal activity is also detected in subsynaptic nuclei in extrafusal muscle fibers.

(B) Low magnification view of the gluteus muscle of a P14 *Pea3*$^{nlslacZ/+}$ mouse processed for β-gal activity. Arrows indicate labeled muscle spindle (S), GTO and the myotendinous junction (MTJ). *Pea3* is also expressed at low levels by Schwann cells associated in intramuscular nerves.

(C) Section through a P10 muscle spindle showing ER81 (red) and AChR (green; αBTX) expression.

(D) β-gal expression in intrafusal muscle fibers in a section of P10 *Er81*$^{nlslacZ/+}$ hindlimb muscle.

(E) ER81 (red) expression by intrafusal muscle fibers and PV^{+} (green) proprioceptive endings in E18 gluteus muscle.

(F) β-gal activity in intrafusal muscle fibers in a section of E18 *Er81*$^{nlslacZ/+}$ hindlimb muscle. Scale bar: (A and B) = 250 μm; (C and E) = 25 μm; (D and F) = 35 μm.

shown). Thus, the temporal profile of ER81 expression in mouse differs from that in chick, where ER81 expression becomes restricted to a subset of proprioceptive neurons by late embryonic stages (Lin et al., 1998).

Expression of ER81 and PEA3 by Muscle Spindles

Intrafusal muscle fibers, a third cell type that contributes to the monosynaptic stretch reflex circuit, are also marked by expression of ER81 and PEA3. Developing intrafusal fibers were identified by expression of Egr3 (Figure 2M; Tourtellotte and Milbrandt, 1998) and by diffuse expression of ACh receptors (Figures 2O, 2P, and 3C). The expression of ER81 and PEA3 in muscle spindles was detected within all limb muscles examined, irrespective of the ETS expression status of the MNs that supply these muscles (Figure 3; see also Figures 8H and 8I; data not shown). PEA3 expression was first detected in muscle spindles at E15.5, but ER81 expression was not detected until E18.0 (Figures 3E and 3F; data not shown). Both proteins were expressed at low or negligible levels by extrafusal muscle fibers (Figures 3A and 3B; data not shown). Cells that contribute to GTOs expressed PEA3 but not ER81 (Figures 3A and 3B; data not shown).

A Defect in Motor Coordination in *Er81* Mutants

To examine the role of *ETS* genes in the development of sensory-motor circuitry, we generated two targeted alleles of *Er81*. In the first allele (*Er81*^{ETS}) the eleventh exon, encoding part of the ETS DNA binding domain, was deleted and in the second allele (*Er81*^{nlslacZ}) an SV40 nuclear localization signal (nls) fused to lacZ was introduced in frame with the ATG present in the second exon (Figure 4A). In mice homozygous for the *Er81*^{ETS} allele, no expression of ER81 protein was detected in DRG or MNs (Figures 4D and 4E), suggesting a null mutation. In the *Er81*^{nlslacZ} allele, no expression of ER81 was detected at E13.5 (data not shown), but from E15, ~5% of the normal number of labeled DRG neurons showed ER81 immunoreactivity (data not shown). The immunoreactivity detected in *Er81*^{nlslacZ} mice, however, is likely to represent an inactive ER81 protein lacking an activation domain (see Experimental Procedures; Coutte et al., 1999). The phenotypes of the *Er81*^{ETS} and *ER81*^{nlslacZ} alleles were similar (data not shown), supporting the idea that both are null mutations.

Mice heterozygous and homozygous for the two targeted *Er81* alleles were born at normal Mendelian frequencies (data not shown) and no overt phenotype was detected in mice heterozygous for either allele. However, mice homozygous for the two *Er81* alleles exhibited marked limb ataxia and abnormal flexor-extensor posturing of their limbs (Figures 4F and 4G; data not shown). This phenotype became apparent in the first few postnatal days and mice died by 3–5 weeks. We have confined our analysis of the *Er81* mutant phenotype primarily to the *Er81*^{ETS} allele, in view of the detection of residual ER81 immunoreactivity in the *Er81*^{nlslacZ} allele.

Motor and Sensory Neurons Are Generated in *Er81* Mutants

The ataxic behavior of *Er81* mutants lead us to examine the development of sensory neurons and MNs. We detected no change in the specification or early differentiation of MNs in *Er81* mutants (Supplemental Figure S1, see Supplemental Data section below). The total number of Isl1^{+} DRG neurons was similar in wild-type and homozygous *Er81*^{ETS} mice (Figures 5A and 5B). The generation

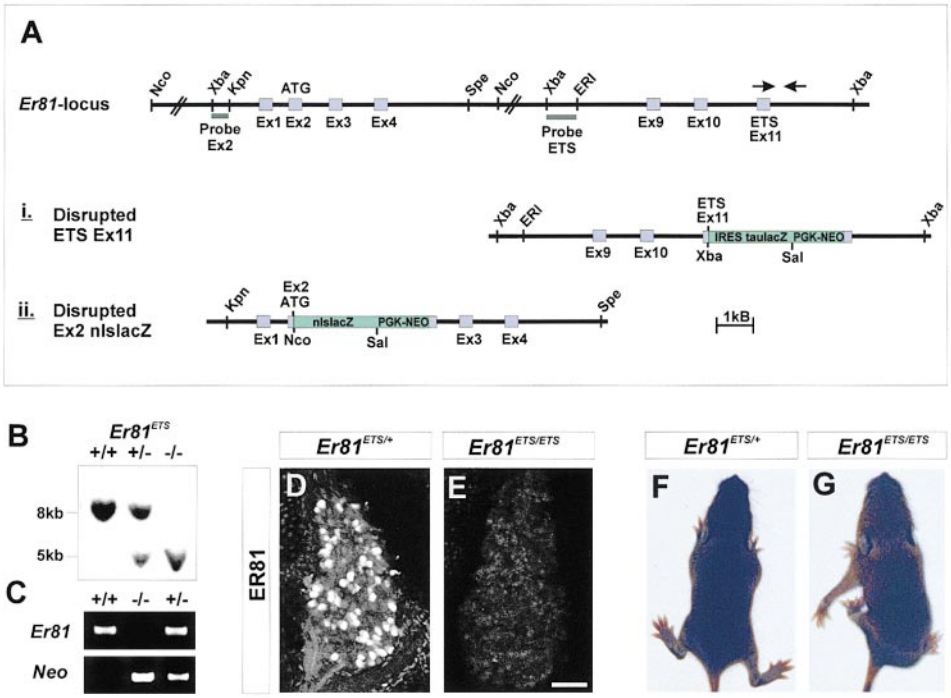

Figure 4. A Motor Coordination Defect in *Er81* Mutant Mice

(A) Generation of *Er81* mutant mice. (Top) Organization of the *Er81* genomic locus in regions targeted by homologous recombination (exons 1–4 and exons 9–11; light blue boxes). Exon 2 contains the *Er81* start codon and exon 11 encodes the N-terminal region of the ETS domain (Coutte et al., 1999). The gray bars indicate the probes (Ex2 and *ETS* Ex11) used to detect homologous recombination in the strategies outlined in (i) and (ii).

(i) Disruption of *Er81* by integration of an *IRES-taulacZpA-PGK-NEO* cassette (Arber et al., 1999) into exon 11. Assay for β-gal activity in these mice indicated that the taulacZ protein was not expressed.

(ii) Integration of a *nlslacZpA-PGK-NEO* cassette into exon 2, in frame with the endogenous ATG (Arber et al., 1999).

(B) Southern blot analysis of $Er81^{ETS}$ mutant mice. Genomic DNA from wild-type (+/+), heterozygous (+/−), and mutant (−/−) tails was digested with XbaI and analyzed with the *ETS* probe (A; ERI/XbaI) detecting an 8 kb wild-type band and a 5 kb mutant band (indicated to the left). Similar diagnostic blots were obtained from the exon 2 targeted allele (available on request).

(C) PCR analysis of genomic DNA from $Er81^{ETS}$ wild-type (+/+), heterozygous (+/−) and mutant (−/−) tails. PCR primers to detect the presence of an unrecombined allele were located in exon 11 (5′primer) and 3′ to exon 11 (3′ primer) to amplify a 500 bp product (arrows in [A] indicate primer positions). This product was absent in $Er81^{ETS}$ mutant mice. Primers within the *Neomycin* gene were used to detect the presence of a targeted allele. An analogous strategy was used to genotype $Er81^{Ex2}$ mutant mice.

(D and E) Absence of ER81 expression in L4/5 DRG of E15.5 $Er81^{ETS}$ mutant mice. The level of protein in DRGs of heterozygous embryos was indistinguishable from that in wild-type embryos.

(F and G) Motor discoordination in $Er81^{ETS}$ mutant mice (P10). Distorted positioning of the forelimb in an $Er81^{ETS}$ mutant but not in wild-type or heterozygous $Er81^{ETS}$ mice.

Scale bar = 30 μm.

of $TrkA^+$ cutaneous neurons was not altered in $Er81^{ETS}$ mutants examined at P5 (data not shown). The number of proprioceptive neurons, assayed by expression of the truncated 5′ *Er81* transcript and by expression of TrkC and lacZ, was similar in wild-type and *Er81* mutant mice from E13 to P5 (Figures 5C–5H, see legend for quantitation). The number of $PEA3^+$ DRG neurons was not altered in $Er81^{ETS}$ mutant mice (data not shown). The number of PV^+ DRG neurons was also similar in wild-type and $Er81^{ETS}$ mutant mice (Figures 5I and 5K), but the level of PV expression in individual neurons was decreased approximately 5- to 10-fold (Figures 5J and 5K). PV^+ axons were also detected in the dorsal roots and peripheral nerves of wild-type, heterozygous, and homozygous $Er81^{ETS}$ mice examined at P5 (Figures 5L–5O), but the level of axonal PV expression was also reduced (data not shown). Thus, with the exception of a decreased level of PV expression, the specification of proprioceptive neurons appears to occur normally in the absence of ER81.

Loss of Monosynaptic Connections between Proprioceptive Afferents and MNs in *Er81* Mutants

To begin to assess the functional properties of proprioceptive neurons in $Er81^{ETS}$ mutants, we stimulated peripheral muscle nerves and recorded compound sensory action potentials in the dorsal root at P6 to P8. Many rapidly conducting proprioceptive afferents were detected in $Er81^{ETS}$ mutants (Figures 5P and 5Q). However, the latency of the fast component of the compound sensory action potential was consistently 1–2 ms longer in $Er81^{ETS}$ mutant mice, and a few axons conducted even more slowly (Figures 5P and 5Q).

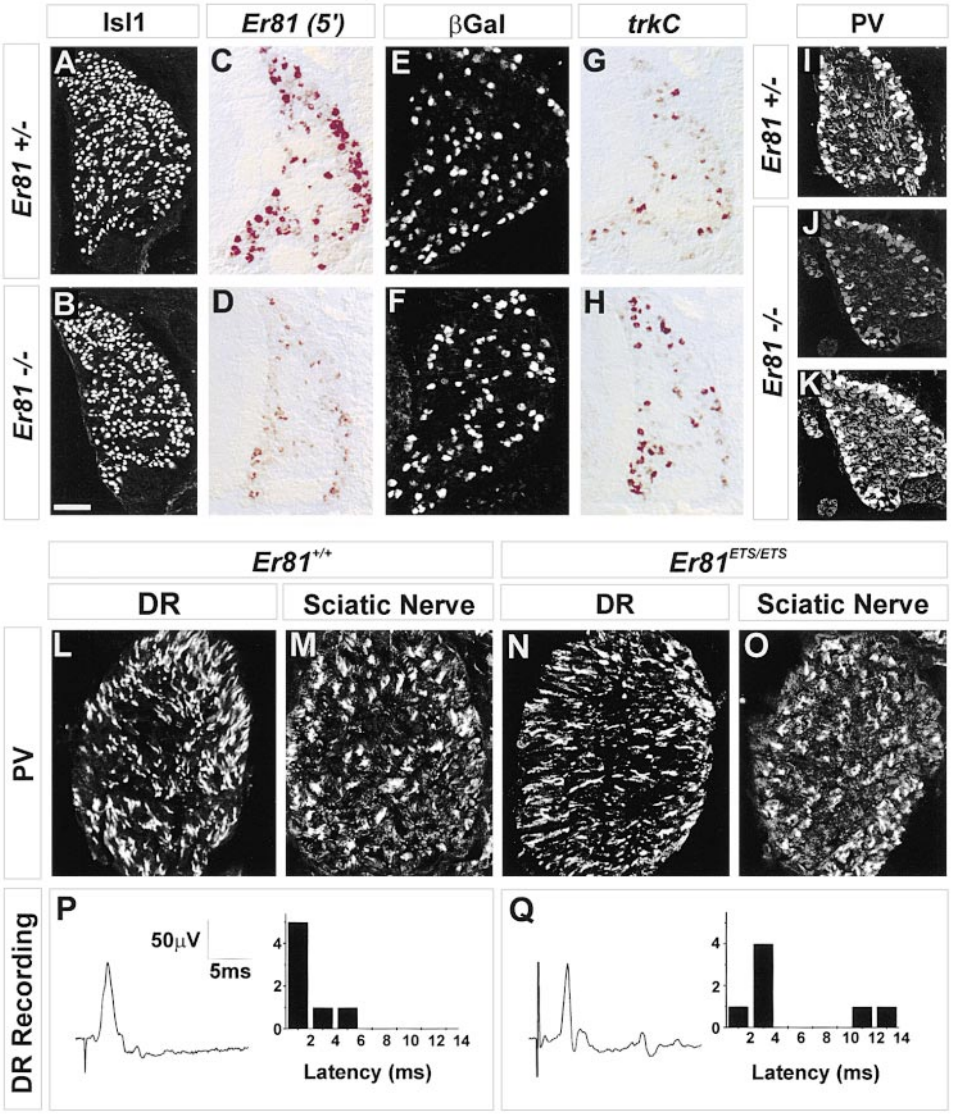

Figure 5. Generation of Proprioceptive Neurons in *Er81*^{ETS} and *Er81*^{nlslacZ} Mutant Mice

(A and B) A similar number of Isl1^{+} DRG neurons is present in *Er81*$^{ETS/+}$ (A) and *Er81*$^{ETS/ETS}$ mutant embryos (B) (E17.5).

(C and D) A 5′ truncated *Er81* transcript is present at low levels in *Er81*$^{ETS/ETS}$ mutant mice. The number of labeled neurons detected in *Er81*$^{ETS/+}$ (C) and *Er81*$^{ETS/ETS}$ mutant mice (D) is comparable.

(E and F) Labeled DRG neurons in *Er81*$^{nlslacZ/+}$ (E) and *Er81*$^{nlslacZ/ETS}$ mutant mice (F). In *Er81*$^{nlslacZ/+}$ (E) mice, the number of β-gal^{+} DRG neurons is similar to that in *Er81*$^{nlslacZ/ETS}$ mice (E13.5) (F). Er81$^{nlslacZ/+}$: 100 +/− 6 β-gal^{+} cells/L4/L5 DRG section; Er81$^{nlslacZ/ETS}$ 101 +/− 10 β-gal^{+} cells/L4/L5 DRG section, E17; mean ± SD; n = 8.

(G and H) *TrkC* expression in P5 mice. The number of neurons detected in *Er81*$^{ETS/+}$ (G) and *Er81*$^{ETS/ETS}$ mutant mice (H) is comparable.

(I–K) Similar numbers of PV^{+} DRG neurons are generated in *Er81*$^{ETS/+}$ (I) and *Er81*$^{ETS/ETS}$ mutant mice (E17.5) (J and K). The level of PV expression in *Er81*$^{ETS/ETS}$ mutant DRGs was reduced by approximately 5- to 10-fold. To estimate the number of PV^{+} neurons in *Er81*$^{ETS/ETS}$ mutant mice, the gain of the confocal microscope was increased (K) to compensate for the reduction in PV expression, achieving a similar signal to that in heterozygotes (I). (Er81$^{ETS/+}$ 992 +/− 88 PV^{+} cells/L4 DRG; 1950 +/− 161 PV^{+} cells/L5 DRG; Er81$^{ETS/ETS}$ 1056 +/− 101 PV^{+} cells/L4 DRG; 1800 +/− 154 PV^{+} cells/L5 DRG; +/+ 1152 + 150 PV^{+} cells/L4 DRG; 1700 +/− 131 PV^{+} cells/L5 DRG. (Mean ± SD; analysis for two embryos of each genotype, counts of every other section).

(L–O) Proprioceptive afferent projections in peripheral nerves and dorsal roots.

Transverse sections through L4 dorsal root (DR; L, *Er81*$^{+/+}$; N, *Er81*$^{ETS/ETS}$) and sciatic nerve (M, *Er81*$^{+/+}$; O, *Er81*$^{ETS/ETS}$). The number of PV^{+} fibers detected in *Er81*$^{+/+}$ (L and M) and *Er81*$^{ETS/ETS}$ mutant mice (N and O) is comparable. The gain of the confocal microscope was increased to collect images in (N) and (O).

(P and Q) Electrical stimulation of the quadriceps muscle nerve at P6 elicits compound sensory action potentials in L3 dorsal roots. The velocity of action potentials is decreased in *Er81*$^{ETS/ETS}$ mutant mice (Q), as indicated in the poststimulation latency histograms.

Scale bars: (A–D, G, and H) = 80 μm; (E and F) = 50 μm; (I–K) = 70 μm; (L–O) = 50 μm.

The mild reduction in axonal conduction velocity observed in *Er81*^{ETS} mutants is unlikely to account for the profound defect in motor coordination. We therefore examined connectivity between proprioceptive afferents and MNs in an isolated spinal cord–peripheral nerve preparation (Mears and Frank, 1997). Low threshold stimuli were applied to dorsal roots or to individual muscle nerves and synaptic responses in MNs were recorded extracellularly from ventral roots.

In wild-type and heterozygous *Er81*^{ETS} mice, dorsal root stimulation elicited compound synaptic responses (Figure 6A; data not shown). The earliest synaptic components, with latencies of 2–3 ms after dorsal root stimulation (black arrowheads in Figure 6), represent monosynaptic input from proprioceptive afferents supplying muscle spindles. This monosynaptic component was sufficiently large to evoke action potentials that were superimposed on the synaptic response of MNs (Figure 6A). Longer latency responses, which reflect polysynaptic proprioceptive and cutaneous sensory input to MNs, were also detected in wild-type and heterozygous mice (Figure 6A). In *Er81*^{ETS} mutants, the amplitude of monosynaptic responses was reduced by ~10 fold, and these inputs were never sufficient to evoke action potentials in MNs (Figure 6B). In contrast, long-latency polysynaptic potentials recorded in *Er81*^{ETS} mutant mice were qualitatively similar to those in wild-type and heterozygous mice (Figures 6A and 6B).

To examine the defect in connectivity in more detail, we recorded synaptic responses in MNs after stimulation of individual muscle and cutaneous nerves. Cutaneous nerve stimulation evoked similar late synaptic responses in wild-type and *Er81*^{ETS} mutant mice (data not shown). In contrast, in *Er81*^{ETS} mutants, monosynaptic inputs elicited by muscle nerve stimulation were greatly reduced (Figures 6C–6J). A reduction in monosynaptic input was observed for all muscle nerves stimulated, independent of whether these nerves supplied muscles innervated by ER81^{+} MNs (obturator, quadriceps; Figures 6C–6F, 6I, and 6J), PEA3^{+} MNs (pectoralis, gluteus; Figures 6G and 6H; data not shown) or ETS^{-} MNs (soleus; data not shown). In *Er81*^{ETS} mutant mice, the decrease in amplitude of the monosynaptic component varied between 4- and 40-fold, depending on the muscle nerve stimulated (Table 1). The reduction in monosynaptic input was evident from P5 to P12, and at all segmental levels (data not shown).

Two features of the response of MNs suggested that the spatial relationship between proprioceptive afferent terminals and MN dendrites is perturbed in *Er81*^{ETS} mutants. First, the rise time of the monosynaptic potential was slower in *Er81*^{ETS} mutants (Figures 6E and 6F), suggesting that inputs are confined to more distal regions of MN dendrites (Kuno and Llinas, 1970). Second, in wild-type mice the synaptic response was preceded by a prepotential (arrows in Figures 6A, 6C, 6E, 6G, and 6I) that reflects the passive response of MN dendrites to local current flow that follows action potential invasion into nearby afferent terminals (Watt et al., 1976). This prepotential was absent in *Er81*^{ETS} mutant mice (Figures 6B, 6D, 6F, 6H, and 6I), suggesting that the density of proprioceptive afferent terminals in the vicinity of MN dendrites is decreased.

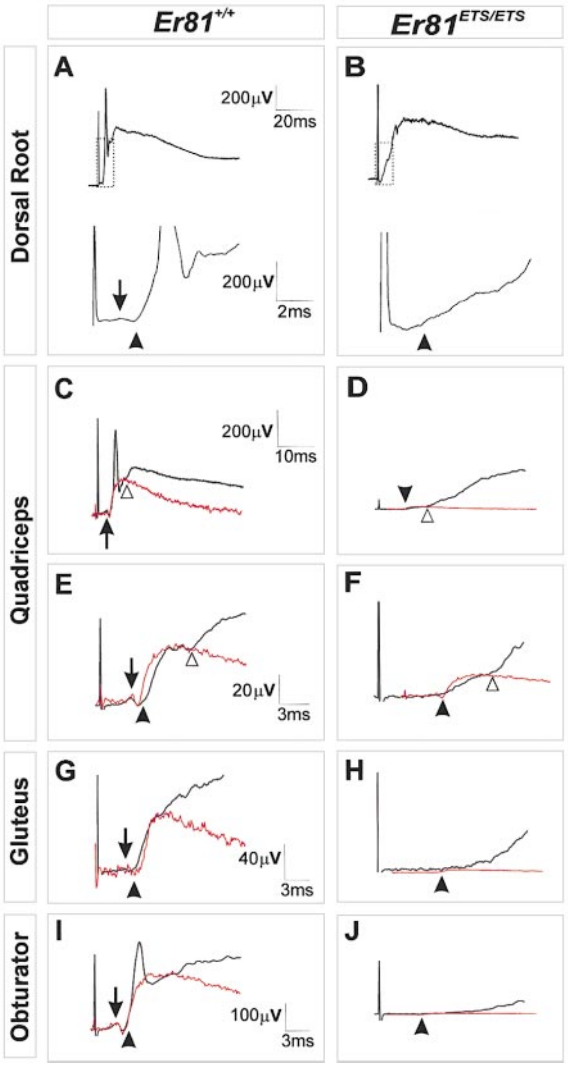

Figure 6. Reduction in Monosynaptic Input from Proprioceptive Afferents to MNs in *Er81* Mutants

(A and B) Stimulation of sensory fibers in the L3 dorsal root at P8 elicits a large ventral root response in both wild-type and *Er81*$^{ETS/ETS}$ mutant animals. Expanded time scale reveals that *Er81*$^{ETS/ETS}$ mutant animals have a greatly reduced response at short latencies, which correspond to monosynaptic afferent input. In wild-type animals (A), the monosynaptic EPSP (which starts at the filled arrowhead in all panels) is suprathreshold, eliciting an action potential in many MNs. In contrast, in *Er81*$^{ETS/ETS}$ mutants, the early component is drastically reduced and is never sufficient to elicit action potentials.

(C–J) Synaptic responses of P8–P9 lumbar MNs to stimulation of low threshold (proprioceptive) afferent fibers in muscle nerves. The monosynaptic component of each response has been fitted with a scaled monosynaptic model trace (red) to estimate its amplitude (see Supplemental Data). With stimulation of the quadriceps or obturator nerves, this component is usually suprathreshold in *Er81*$^{ETS/+}$ or wild-type mice (C and I; data not shown), but is substantially reduced in *Er81*$^{ETS/ETS}$ mutant mice (D, F, H, and J). Polysynaptic afferent input, which begins where the response deviates from the model trace (open arrowheads) is still present in *Er81*$^{ETS/ETS}$ mutant mice. Proprioceptive afferent inputs in *Er81*$^{ETS/ETS}$ mutant mice also have longer latencies. Two other characteristic features of proprioceptive inputs in *Er81*$^{ETS/ETS}$ mutant mice, the absence of prepotentials (vertical arrows in A, C, E, G, and H) and the slower rising phase of the residual monosynaptic component (compare E and F) are discussed in the text.

Table 1. Reduction of Monosynaptic Sensory-Motor Potentials in Response to Muscle Nerve Stimulation in *Er81*^{ETS} Mutant Mice

Peripheral Nerve	*Er81*$^{+/+}$	*Er81*$^{ETS/ETS}$	% Normal
Quadriceps	179.6 ± 24.6 (16)	15.4 ± 3.2 (12)	8.6
Obturator	182.3 ± 20.9 (9)	4.4 ± 0.8 (8)	2.4
Gluteus	65.1 ± 14.8 (4)	1.7 ± 0.2 (4)	2.6
MBS	141.0 ± 25.5 (7)	10.2 ± 3.5 (6)	7.2
Peroneal	117.6 ± 26.3 (7)	25.7 ± 3.9 (7)	21.9
Tibial	229.4 ± 36.5 (7)	61.8 ± 12.6 (7)	26.9

Average amplitude of monosynaptic potentials recorded from ventral roots after stimulation of individual muscle nerves at P5 to P10. The reduction in EPSP amplitude is significantly reduced in *Er81*^{ETS} mutants for all muscle nerves examined ($p < 0.05$, Student's t test). Amplitude in μV, mean ± SEM, number of experiments indicated in parentheses.

An Anatomical Defect in the Termination of Proprioceptive Afferents in *Er81* Mutants

The physiological defect in sensory-motor connectivity in *Er81*^{ETS} mutants led us to examine whether there is a detectable change in the intraspinal projection of proprioceptive afferents and if so, when this defect becomes apparent. We used two assays to trace the intraspinal projection and termination zones of proprioceptive axons. HRP was injected into the dorsal roots of embryonic and postnatal mice, and the projection of afferents supplying muscle or cutaneous targets was traced (Figures 7A–7H). The projection of proprioceptive afferents was also assessed by axonal expression of TrkC or PV (Figures 7I–7P).

In wild-type embryos, proprioceptive afferents project into the dorsal spinal cord at E14.0 (Ozaki and Snider, 1997), and by E15.0 have projected to the intermediate zone, close to a set of Isl1^{+} neurons located in the deep dorsal horn (Figures 7A and 7I; data not shown). Between E15.5 and P0, group Ia muscle spindle afferents project further ventrally, close to proximal MN dendrites and MN cell bodies (Figures 7C and 7K). By E18 to P2, muscle spindle afferents have formed direct functional connections with MNs (Mears and Frank, 1997). In contrast, proprioceptive afferents supplying GTOs (group Ib afferents) project only to the intermediate spinal cord and solely contact interneurons (Brown, 1981).

At E14.0 to E15.5, the projection of proprioceptive afferents into the dorsal spinal cord, assessed by TrkC expression and HRP labeling, was similar in wild-type, heterozygous, and homozygous *Er81*^{ETS} embryos (Figures 7A, 7B, 7I, and 7J; data not shown). From E16.0, however, the ventral termination zone characteristic of group Ia afferents was almost completely absent in *Er81*^{ETS} mutants (Figures 7D, 7F, 7H, 7L, 7N, and 7P). Fewer than 1% of the normal number of HRP-labeled and PV^{+} proprioceptive afferents were detected ventral to the position of Isl1^{+} interneurons (Figure 7D; data not shown). The density of proprioceptive afferent projections in the dorsal and intermediate spinal cord, however, appeared similar in wild type and *Er81*^{ETS} mutants examined at E15.0 to E16.5 (Figures 7A–7D, 7I, and 7J). A similar defect was observed at forelimb and thoracic levels (data not shown). No change in the central projections of cutaneous afferents in the dorsal spinal cord was detected, assessed by HRP tracing (Figures 7A and 7H) and Neuropilin-1 expression (Supplemental Figure S2). Thus, in *Er81*^{ETS} mutants, proprioceptive neurons fail to form a ventral termination zone characteristic of group Ia afferents. As a consequence, the extent of overlap between proprioceptive afferents and MN dendrites is markedly reduced, leading to the reduction in monosynaptic connectivity detected physiologically.

A Defect in Muscle Spindle Differentiation in *Er81* Mutants

We also examined whether the peripheral connections of proprioceptive afferents are defective in *Er81*^{ETS} mutants. To test this, we analyzed molecular markers of differentiated muscle spindles and GTOs and used physiological methods to assess the activation of group Ia and group Ib sensory endings. The differentiation and function of GTOs examined at P5–P10 was not obviously affected in *Er81* mutants (see Supplemental Figure S3).

In *Er81*^{ETS} mutants, the differentiation of muscle spindles was initiated, as assessed by expression of Egr3 at E15 to E18.0 (Figures 8A and 8D; data not shown), and by the presence of PV^{+}, GAP43^{+} proprioceptive axons (Figures 8B, 8C, 8E, and 8F; data not shown). However, between E18 and P5 there was a clear defect in the differentiation of intrafusal fibers, assessed by the loss of expression of Egr3 and of the *Er81*^{nlslacZ} marker (Figures 8G–8L). The extent of the loss of differentiated intrafusal fibers, however, varied between individual muscle groups (Figures 8H, 8I, 8K, and 8L). The number of PV^{+} axons within the muscle mass was also markedly reduced (data not shown), but it is unclear whether this reflects the retraction of proprioceptive axons or the loss of PV expression.

We also examined the activation of group Ia afferents with stimuli (vibration) that selectively activate muscle spindles (Brown et al., 1967). In wild-type mice examined at P5–P10, vibration of the quadriceps muscle elicited a nearly synchronous firing of several group Ia fibers (Figure 8M). Group Ia fiber responses followed stimulus frequencies of 50 Hz (Figure 8O). In contrast, in *Er81*^{ETS} mutant mice, muscle vibration was much less effective in activating group Ia afferent fibers (Figures 8N and 8P), and in ~50% of mutant mice, group Ia fiber activity was absent (Figure 8P; data not shown). Together, these results indicate that the loss of ER81 function leads to a late defect in the development and function of muscle spindles.

Discussion

This study provides genetic evidence that ER81 is required for the formation of functional connections between proprioceptive afferents and MNs. In *Er81* mutants, group Ia muscle spindle afferents fail to establish

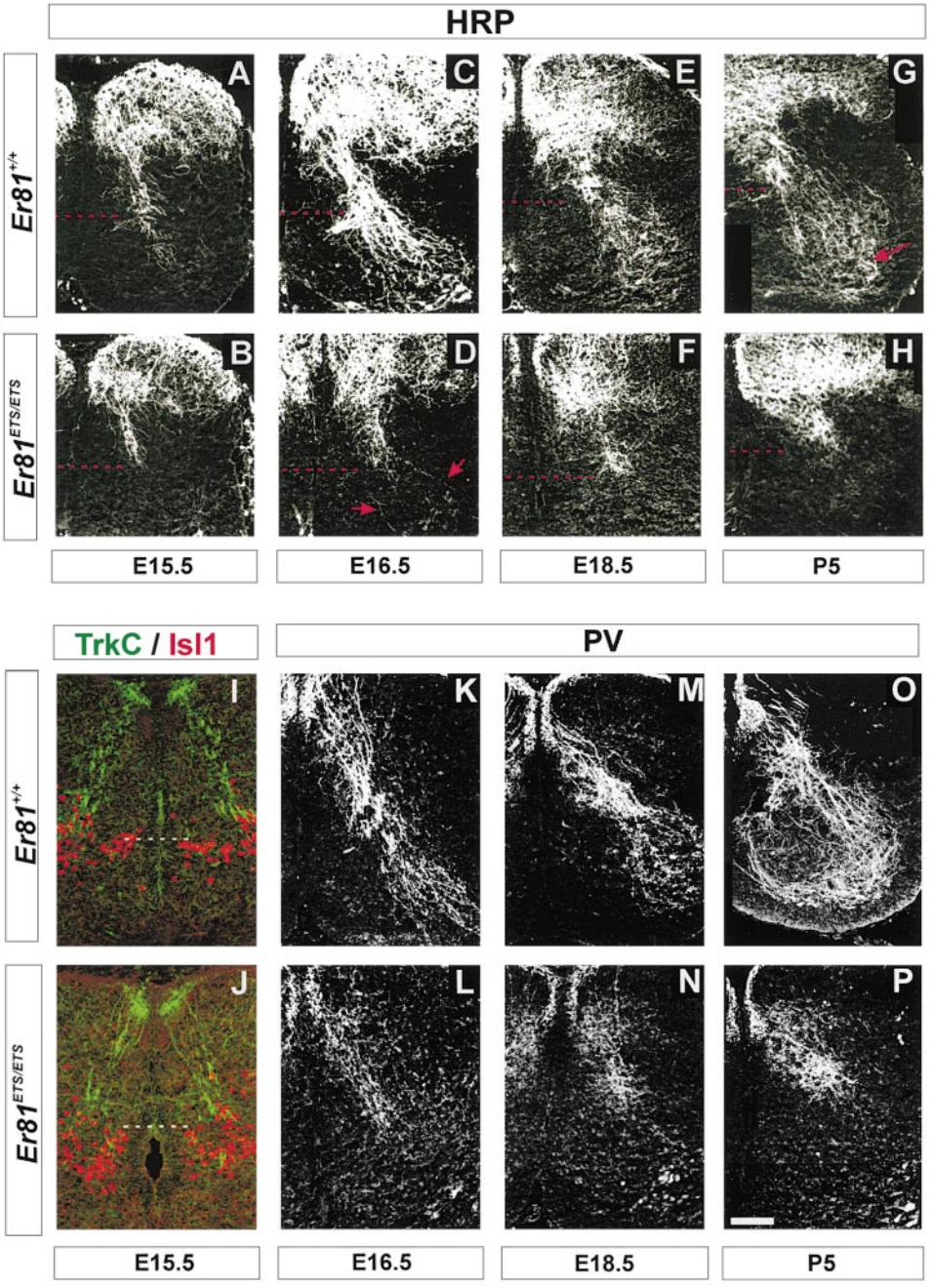

Figure 7. A Defect in the Central Projection of Proprioceptive Afferents in *Er81*^{ETS} Mutants

(A–H) Development of the sensory afferent projections into the spinal cords of wild type (A, C, E, and G) and *Er81*$^{ETS/ETS}$ mutant (B, D, F, and H) mice assessed after HRP injections into L4/5 DRGs (E15.5 and E16.5) or L4/5 dorsal roots (E18.5 and P5). The red dashed lines indicate the dorsoventral position of Isl1^{+} interneurons (I; data not shown). Red arrows in (D) indicate some of the very few proprioceptive afferents that extend into the ventral spinal cord in *Er81*^{ETS} mutants. Arrow in (G) indicates the region of MN cell bodies. This region is devoid of proprioceptive afferent fibers in *Er81*$^{ETS/ETS}$ mutant mice (H).

(I and J) At E15.5, TrkC^{+} afferent fibers (green) project into the dorsal spinal cord (L4/5) reaching the position of dorsal Isl1^{+} interneurons (red) in similar numbers in *Er81*$^{+/+}$ (I) and *Er81*$^{ETS/ETS}$ mutant (J) embryos.

(K–P) Development of proprioceptive afferent projections in *Er81*$^{+/+}$ (K, M, and O) and *Er81*$^{ETS/ETS}$ mutant (L, N, and P) mice at L4/5, assessed by PV expression at E16.5 (K and L), E18.5 (M and N) and P5 (O and P). The level of PV expression in *Er81*^{ETS} mutant spinal cords was reduced by approximately 5- to 10-fold but was compensated for by enhancing the gain of confocal images.

Scale bar: (A–D) = 100 μm; (E–H) = 160 μm; (I and J) = 60 μm; (K and L) = 100 μm; (M–P) = 170 μm.

a characteristic ventral termination zone in the vicinity of MN dendrites and as a consequence functional reflex motor output is abolished. We discuss these findings in context of the role of transcription factors in the assembly of neuronal circuits in the developing vertebrate CNS.

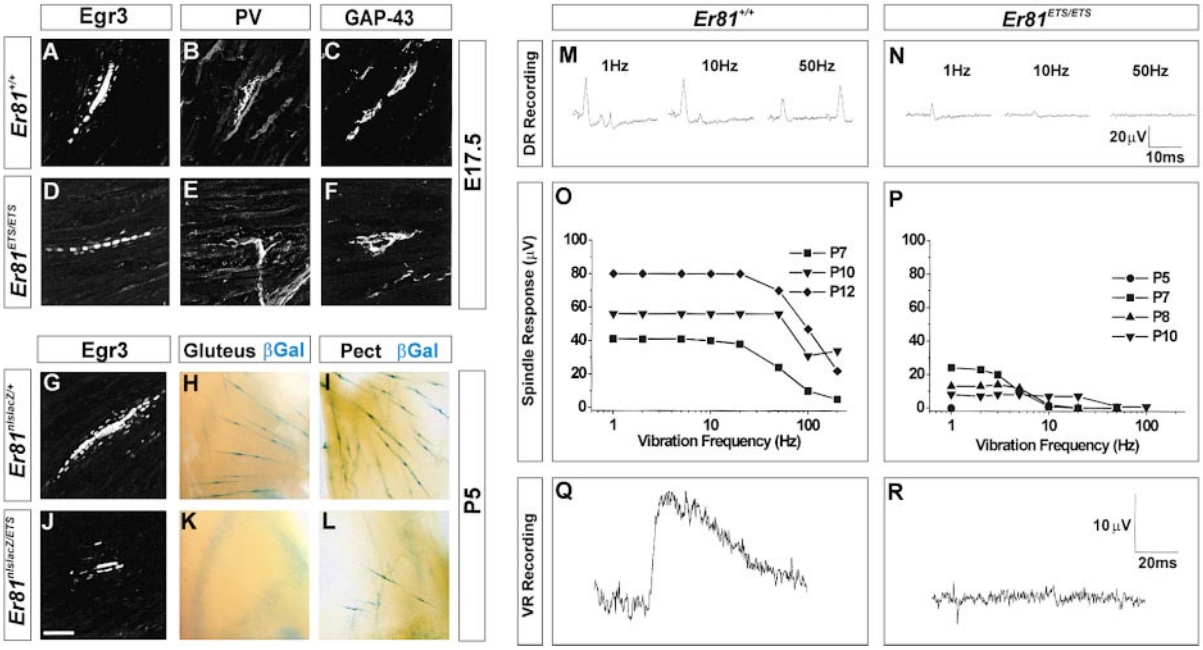

Figure 8. A Defect in the Development of Muscle Spindles in *Er81*^{ETS} Mutants

(A–F) The initial stages of muscle spindle differentiation occur in *Er81*$^{ETS/ETS}$ mutant mice. Serial sections through the same muscle spindle in *Er81*$^{+/+}$ (A–C) and *Er81*$^{ETS/ETS}$ mutant (D–F) embryos (E17.5), stained to reveal Egr3 (A and D) and PV^{+} (B and E) or GAP-43^{+} (C and F) axons.

(G–L) A defect in muscle spindle differentiation at P5 in *Er81*$^{ETS/ETS}$ mutant mice.

(G and J) A muscle spindle in the quadriceps muscle stained to reveal Egr3 in *Er81*$^{nlslacZ/+}$ (G) and *Er81*$^{nlslacZ/ETS}$ mutant (J) mice.

(H–L) Whole mount view of gluteus (H and K) and pectoralis (I and L) muscle in a *Er81*$^{nlslacZ/+}$ (H and J) or *Er81*$^{nlslacZ/ETS}$ (K and L) mouse (P7) processed for β-gal activity. The loss of molecular markers of intrafusal muscle fibers was virtually complete in the gluteus, gracilis, biceps femoris, and semitendinosus muscles, whereas residual spindles were detected in the pectoralis, adductor, rectus femoris and some other muscles.

(M–R) Activation of group Ia afferents and synaptic responses elicited in MNs.

(M–P) Selective stimulation of group Ia afferents in the RF head of quadriceps. Group Ia afferents in both *Er81*$^{+/+}$ (M and O) and *Er81*$^{ETS/ETS}$ mutant (N and P) mutant mice respond to low-frequency vibration during the first postnatal week. However, the response in *Er81*$^{ETS/ETS}$ mutant mice is defective: fewer spindle afferents are activated and most afferents that do respond cannot follow vibration frequencies >20 Hz. A single Ia afferent produced a ~10 μV response in both wild-type and *Er81*$^{ETS/ETS}$ mutants.

(Q and R) Synaptic responses recorded after peripheral activation of group Ia axons recorded in L3 ventral root in *Er81*$^{+/+}$ (Q) and *Er81*$^{ETS/ETS}$ mutant (R) mice (P6–P7). Selective activation of quadriceps group Ia fibers elicits a subthreshold monosynaptic potential with no prominent late components in *Er81*$^{+/+}$ mice (Q). No response is detected in *Er81*$^{ETS/ETS}$ mutants (R).

Scale bar: (A–F) = 40 μm; (G and J) = 60 μm; (H, I, K, and L) = 300 μm.

Specification of Proprioceptive Neurons and MNs Is Independent of ER81 Function

The onset of ER81 expression normally occurs at a relatively late stage in the specification of sensory and MN identity—after MNs have acquired their columnar and rostrocaudal identity (Goulding, 1998) and after DRG neurons express molecular markers of proprioceptive and cutaneous neuronal subclasses (Farinas et al., 1998; Ma et al., 1999). Since ER81 expression occurs only after axons have entered the periphery, and early limb ablation prevents the onset of neuronal *Er81* expression (Lin et al., 1998), signals from the limb may control the onset of ETS gene expression.

Consistent with the late onset of ER81 expression, *Er81* mutant mice do not show any defect in the specification of MNs or in the projection of MNs to individual muscles in the limb. Moreover, the initial guidance of proprioceptive axons along the dorsal roots and into the dorsal spinal cord is unchanged in *Er81* mutants. Thus, the loss of *Er81* function does not perturb the guidance of the axons of MNs or proprioceptive neurons in the periphery or into the dorsal spinal cord.

A Central Defect in Sensory-Motor Connectivity in *Er81* Mutants

The first detectable defect in *Er81* mutants is a failure of proprioceptive afferents to establish a ventral termination zone, a hallmark of group Ia muscle spindle afferents. Nevertheless, some proprioceptive afferents in *Er81* mutants still terminate close to the distal region of MN dendrites in the intermediate spinal cord (Ozaki and Snider, 1997).

Is the loss of the ventral termination zone of proprioceptive axons sufficient to explain the pronounced loss of monosynaptic connectivity in *Er81* mutants? Fewer than 1% of the normal number of proprioceptive afferents invade the ventral spinal cord in *Er81* mutants. Despite this, for some muscle nerves, the monosynaptic input from proprioceptive afferents to MNs in *Er81* mutants was up to 25% of that detected in wild-type or heterozygous mice (Table 1). Moreover, the pronounced slowing in the rise time of the monosynaptic potentials recorded in *Er81* mutants indicates that residual afferent synaptic contacts are established primarily on the distal region of MN dendrites (Kuno and Llinas, 1970). To-

gether, these observations suggest that those proprioceptive afferents that find themselves in the vicinity of distal MN dendrites in *Er81* mutants are still able to establish monosynaptic connections. Thus, ER81 appears to control the formation of a ventral afferent termination zone rather than the process of synaptogenesis itself.

An Intrinsic Requirement for ER81 in Proprioceptive Neurons

The expression of ER81 by proprioceptive neurons, MNs, and intrafusal muscle fibers complicates assignment of the cellular locus of ER81 action that underlies the defect in afferent termination zone. Nevertheless, the expression of ER81 by MNs is unlikely to be responsible for the defect in afferent projections, since the loss of the ventral termination zone and monosynaptic connectivity are evident at forelimb levels of the spinal cord where few if any MNs express ER81. Signals from muscle spindles have been suggested to influence the development of proprioceptive afferents (E. Frank et al., Soc. Neurosci. abstract *25*, 2011, 1999). In particular, mice lacking the function of Egr-3, exhibit a postnatal degeneration of muscle spindles (Tourtellotte and Milbrandt, 1998; J. Kucera et al., Soc. Neurosci. abstract *25*, 2011, 1999) and monosynaptic input from proprioceptive afferents to MNs is reduced (E. Frank et al., Soc. Neurosci. abstract *25*, 2011, 1999). However, the loss of expression of ER81 from muscle spindles cannot initiate the proprioceptive axonal projection defect. ER81 is first expressed in muscle spindles only at E18, well after the proprioceptive afferent projection defect is evident. Together, these findings indicate that proprioceptive neurons represent the primary locus of action of ER81.

Proprioceptive neurons can be divided into two major classes; group Ia and group Ib afferents. The density of proprioceptive afferents observed in the dorsal spinal cord is similar in *Er81* mutants and wild-type embryos, suggesting that all proprioceptive afferents project as far as the intermediate spinal cord. The detection of residual monosynaptic connections between proprioceptive afferents and MNs in *Er81* mutants also indicates that some functional group Ia afferents are present in the intermediate spinal cord. But in the absence of ER81, all proprioceptive afferents terminate in a pattern characteristic of group Ib afferents. Thus, ER81 function appears to be required to establish the distinct laminar termination zones of group Ia and group Ib proprioceptive afferents. Why then do group Ib afferents normally fail to project into the ventral spinal cord, since they also express ER81? Our results imply that ER81 is inactive in group Ib afferents, perhaps because this set of neurons lacks an essential cofactor, or expresses an inhibitor of ER81 function.

At early developmental stages, ER81 and PEA3 are coexpressed by many proprioceptive neurons, raising the issue of potential redundancy between these two genes. PEA3 clearly does not substitute for ER81 in establishing the ventral termination zone of proprioceptive afferents. Nevertheless, ER81 and PEA3 could, in principle, have redundant functions in controlling the initial trajectory of proprioceptive afferents in the dorsal spinal cord. Against this idea, the proprioceptive afferent projection phenotype observed in *Pea3, Er81^{ETS}* double mutant embryos is not more severe than that in *Er81^{ETS}* mutants (S. A. and T. M. J., data not shown). Thus, ER81 and PEA3 appear to have nonredundant functions in proprioceptive neurons, perhaps a consequence of differences in their preferred target DNA sequences (Mo et al., 1998).

ETS Gene Expression and Muscle Spindle Development

The initial steps of muscle spindle development occur in *Er81* mutant mice, but many intrafusal fibers subsequently dedifferentiate or degenerate. The loss of differentiated muscle spindles in *Er81* mutants could provide an explanation for the slowed conduction velocity of proprioceptive afferents. It remains unclear, however, whether the muscle spindle phenotype observed in *Er81* mutants reflects the loss of expression of ER81 from muscle spindles or from proprioceptive neurons. In principle, the muscle spindle defect could result from the loss of a factor supplied by proprioceptive neurons that is necessary for the maintenance of muscle spindles. Nevertheless, in *Er81* mutants, pronounced defects in muscle spindle development occur only after the normal onset of ER81 expression by intrafusal fibers, suggesting that ER81 expression may be required in intrafusal muscle fibers themselves.

The loss of the differentiated properties of intrafusal fibers in *Er81* mutants is not evident in all muscle groups. Other studies have provided evidence for heterogeneity in the neurotrophic factor dependence of muscle spindles in different muscle groups (Kucera et al., 1998; J. Kucera et al., Soc. Neurosci. abstract *25*, 2011, 1999). The differential loss of muscle spindles observed in *Er81* mutants could contribute to the variability in the extent of residual monosynaptic connectivity between different sets of proprioceptive neurons and MNs (Table 1).

ETS Gene Expression and the Selectivity of Sensory-Motor Connections

Studies in chick have revealed a matching in the expression of ER81 and PEA3 in interconnected sensory and MNs (Lin et al., 1998). This finding raised the possibility that *ETS* genes control aspects of pool-specific sensory-motor connectivity. The severity of the connectivity defect in these constitutive *Er81* mutants has prevented us from analyzing directly the role of ETS proteins in establishing specific sensory-motor connections.

Comparison of the pattern of ER81 expression in mouse and chick also reveals a divergence in its regulation by proprioceptive neurons. A common early phase of widespread ER81 expression in mouse is not followed by protein segregation into distinct sensory neuron pools, as in chick. This finding reduces the likelihood that the expression of ER81 in sensory neurons contributes to the specificity of proprioceptive afferent connections with individual motor pools in the mouse. However, in mouse the level of ER81 protein varies markedly in different proprioceptive neurons, and ER81 isoforms with differing activities can be generated through alternative splicing and differential phosphorylation (Wasylyk et al., 1998; Coutte et al., 1999). It remains possible,

therefore, that different subsets of proprioceptive neurons in the mouse do exhibit different levels of ER81 activity. Independent of this issue, our results do not negate a role for ER81 in defining the specificity of proprioceptive afferent connections with MN pools, by virtue of the selective and conserved expression of the protein in specific MN pools.

Neuronal Circuit Assembly and Transcription Factors

Our studies indicate that ER81 has a selective role in establishing the distinct laminar termination zone that characterizes one of the two major subclasses of proprioceptive afferent neurons, without any earlier influence on the guidance of sensory or motor axons. This distinction in afferent termination zone is critical for the formation of functional sensory-motor circuits. In this sense, the role of ER81 revealed here contrasts with the actions of many other transcription factors that regulate either neuronal fate or early steps in axon guidance (Bang and Goulding, 1996; Landgraf et al., 1999; Sauereissig et al., 1999; Thor et al., 1999).

Recent analysis of mice lacking *Otx1* function has shown that certain cortical neurons fail to refine their exuberant axonal projections (Weimann et al., 1999), but it remains unclear if *Otx1* controls the connectivity of those cortical projections that are normally preserved. The function of *Er81* revealed in this study does, however, suggest parallels with the role proposed for *Unc-4*, a homeobox gene that appears to dictate the selectivity of synaptic input from interneurons to MNs in *C. elegans* (Miller and Niemeyer, 1995). Analysis of the molecular targets of ER81 in proprioceptive neurons may provide further insight into the way in which ETS transcription factors define late steps in the assembly of neuronal circuits in the mammalian CNS.

Experimental Procedures

Generation of *Er81* Mutant Mice

Mouse genomic clones were derived from a 129/Sv genomic library (Stratagene). For details on the genomic structure of the mouse *Er81* locus see GenBank accession AF109633 to AF109642 (Coutte et al., 1999). The targeting vector for production of the $Er81^{ETS}$ allele was constructed from an 8.5 kb EcoRI/XbaI genomic fragment containing 5.5 kb sequence 5′ to exon 11, 3 kb 3′ to exon 11, and a 5′ PmeI site. An XbaI site followed by stop codons in all three reading frames and a PacI site for insertion of the IRES-taulacZ cassette (Arber et al., 1999) were integrated into exon 11. The probe used to screen ES cell recombinants was a 1 kb XbaI/EcoRI 5′ region (XbaI digest). Oligonucleotides used for PCR screening (500 bp band) were: 5′-ATTTCATTGCCTGGACTGGACGAG-3′ and 5′-TCACTCACAGAATGTTGTCTCTCC-3′. The targeting vector for the production of the $Er81^{nlslacZ}$ allele was derived from a 7 kb KpnI/SpeI fragment. Targeting cassettes (Arber et al., 1999; without an IRES) were integrated in frame with the endogenous ATG by insertion of an NcoI site into exon 2. The probe used to screen ES cell recombinants was a 400 bp XbaI/KpnI 5′ region (NcoI digest). PmeI linearized targeting constructs were electroporated into W95 ES cells, selected with G418 and screened by Southern blot analysis. The frequency of recombination was ~1:5 (exon 11 construct) and ~1:30 (exon 2 construct). Recombinant clones were injected into C57BL/6J blastocysts to generate chimeric founders that transmitted the mutant allele. All experiments involved analysis of embryos or offspring derived from heterozygous 129Sv × C57BL/6J intercrosses. Findings reported in this paper are based on analysis of over 100 $Er81^{ETS}$ mutant embryos and neonates. Information on the generation of $Pea3^{nlslacZ}$ and $Pea3^{taulacZ(3')}$ lines is available upon request. $Hb9^{nlslacZ}$ mice have been described (Arber et al., 1999).

In Situ Hybridization and Immunocytochemistry

Cryostat sections were hybridized with digoxigenin-labeled mouse *Er81* and rat *TrkC* probes as described (Schaeren-Wiemers and Gerfin-Moser, 1993). Most antibodies used have been described (Arber et al., 1999); rabbit and guinea pig anti-ER81 were generated against the 11 C-terminal aa of mouse ER81. Other antibodies were anti-TrkA (Huang et al., 1999); anti-PV (Swant); anti-TSP4 (Arber and Caroni, 1995); anti-S100 (DAKO); anti-Egr-3 (O'Donovan et al., 1998); goat anti-TrkC (Huang et al., 1999). Immunocytochemistry was performed as described (Kopp et al., 1997; Arber et al., 1999) using fluorophore-conjugated secondary antibodies (Jackson Labs) (1:500 to 1:1000). Rhodamine-labeled α-bungarotoxin (Jackson Labs) was used at 1:2000. Images were collected on a BioRad MRC 1024 confocal microscope.

Retrograde Neuronal Labeling and Histochemistry

To trace the projection of sensory afferents, the spinal cord was exposed leaving the dorsal roots and DRG intact. HRP was injected into DRGs (E15 to E16.5) or dorsal roots (embryos older than E16.5) using glass capillaries. After injection, embryos were incubated for 2–3 hr (Lin et al., 1998; Arber et al., 1999) before fixation and detection of HRP. For retrograde tracing, HRP was injected into limb muscles of E15.5 embryos and incubated for 4 hr (Lin et al., 1998). Cholera toxin-HRP (0.1% in PBS; List Biological Laboratories) was injected into the quadriceps nerve in vivo at P3 and animals were processed for HRP activity after 3 days (Rivero-Melian, 1996). β-galactosidase staining was performed as described (Arber et al., 1999).

Electrophysiological Analysis

Spinal cords with attached peripheral nerves, and in some cases with the quadriceps muscle group, were isolated at P5 to P10 and maintained as described (Mears and Frank, 1997). Extracellular recordings from motor and sensory neurons were made at 25°C with suction electrodes applied to ventral and dorsal roots. Group Ia axons were activated selectively by applying 1–2 ms ~50 μm stretches to the distal tendon of the RF head with a piezoelectric bimorph (Brown et al., 1967; Lichtman and Frank, 1984). For activating group Ib axons selectively, we elicited single twitch contractions of RF via electrical stimulation (below threshold for γ fiber activation) of the L3 ventral root (Jansen and Rudjord, 1964). Synaptic potentials were measured from averages of 10–20 traces at 0.5 Hz. No significant differences were noted between heterozygous and wild-type mice.

The monosynaptic (group Ia) component of synaptic responses was estimated by scaling a superimposed model trace of proprioceptive input from the same muscle in a normal mouse of similar age (Mears and Frank, 1997). The model trace was evoked by stimulating a muscle nerve at just suprathreshold strength; the resulting small (10–20 μV) synaptic potential therefore included few, if any, polysynaptic components. For responses in mutant mice, the model was delayed by 1–3 ms to allow for the longer peripheral conduction times of the afferents, which were measured as in Figures 5P and 5Q. When inputs were suprathreshold (Figures 6C and 6I), the true amplitude of the monosynaptic components in those MNs with spikes was probably underestimated because their peaks occurred just after the action potential. Since suprathreshold inputs were never observed in mutant mice, however, this error would lead only to an underestimate of the reduction of responses in mutants. Rise times were measured between 5% and 95% of peak amplitude. When responses were superthreshold, the stimulus intensity was reduced to obtain a subthreshold response.

Supplemental Data

Supplemental text and Figures S1–S3 are available online (http://www.cell.com/cgi/content/full/101/5/485/DC1).

Acknowledgments

We thank M. Smith for technical assistance, B. Han and M. Mendelsohn for help in the generation of mutant mice, and S. Morton for

help in antibody generation. We are grateful to L. Reichardt and L. Parada for Trk reagents, H. Fujisawa for anti-Neuropilin antibodies, D. Kopp for advice on identification of GTOs, J. Kucera for insights into muscle spindle development and J. Hassell for discussion of *ETS* gene function. R. Axel, P. Caroni, J. De Nooij, K. Lee, S. Price, N. Shah, and N. Shneider provided comments on the manuscript. We thank K. MacArthur for help in preparing the manuscript. S. A. is supported by a HFSP Fellowship and a grant from the Swiss National Science Foundation. E. F. and D. L. are supported by grants from the NIH. T. M. J. is supported by grants from the NIH and is an Investigator of the HHMI.

Received February 1, 2000; revised April 18, 2000.

References

Arber, S., and Caroni, P. (1995). Thrombospondin-4, an extracellular matrix protein expressed in the developing and adult nervous system promotes neurite outgrowth. J. Cell Biol. *131*, 1083–1094.

Arber, S., Han, B., Mendelsohn, M., Smith, M., Jessell, T.M., and Sockanathan, S. (1999). Requirement for the homeobox gene *Hb9* in the consolidation of motor neuron identity. Neuron *23*, 659–674.

Bang, A.G., and Goulding, M.D. (1996). Regulation of vertebrate neural cell fate by transcription factors. Curr. Opin. Neurobiol. *6*, 25–32.

Brown, A.G. (1981). Organization in the Spinal Cord (New York: Springer), pp. 154–214.

Brown, M.C., Engberg, I., and Matthews, P.B.C. (1967). The relative sensitivity to vibration of muscle receptors of the cat. J. Physiol. (Lond.) *192*, 773–800.

Cepko, C.L. (1999). The roles of intrinsic and extrinsic cues and bHLH genes in the determination of retinal cell fates. Curr. Opin. Neurobiol. *9*, 37–46.

Chen, H.H., and Frank, E. (1999). Development and specification of muscle sensory neurons. Curr. Opin. Neurobiol. *9*, 405–409.

Coutte, L., Monte, D., Imai, K., Pouilly, L., Dewitte, F., Vidaud, M., Adamski, J., Baert, J.L., and de Launoit, Y. (1999). Characterization of the human and mouse ETV1/ER81 transcription factor genes: role of the two alternatively spliced isoforms in the human. Oncogene *4*, 6278–6286.

Eccles, J.C., Eccles, R.M., and Lundberg, A. (1957). The convergence of monosynaptic excitatory afferents onto many different species of alpha motoneurones. J. Physiol. (Lond.) *137*, 22–50.

Farinas, I., Wilkinson, G.A., Backus, C., Reichardt, L.F., and Patapoutian, A. (1998). Characterization of neurotrophin and Trk receptor functions in developing sensory ganglia: direct NT-3 activation of TrkB neurons in vivo. Neuron *21*, 325–334.

Frank, E., Smith, C., and Mendelson, B. (1988). Strategies for selective synapse formation between muscle sensory and motor neurons in the spinal cord. In From Message to Mind, S.S. Easter, K.F. Barald, and B.M. Carlson, eds. (Sunderland, MA: Sinauer Associates Inc.), pp. 180–202.

Goulding, M. (1998). Specifying motor neurons and their connections. Neuron *21*, 943–946.

Honda, C.N. (1995). Differential distribution of calbindin-D28k and parvalbumin in somatic and visceral sensory neurons. Neuroscience *68*, 883–892.

Huang, E.J., Wilkinson, G.A., Farinas, I., Backus, C., Zang K., Wong, S.L., and Reichardt, L.F. (1999). Expression of Trk receptors in the developing mouse trigeminal ganglion: in vivo evidence for NT-3 activation of TrkA and TrkB in addition to TrkC. Development *126*, 2191–2203.

Jansen, J.K.S., and Rudjord, T. (1964). On the silent period and Golgi tendon organs of the soleus muscle of the cat. Acta Physiol. Scand. *62*, 364–379.

Kopp, D.M., Trachtenberg, J.T., and Thompson, W.J. (1997). Glial growth factor rescues Schwann cells of mechanoreceptors from denervation-induced apoptosis. J. Neurosci. *17*, 6697–6706.

Kucera, J., Fan, G., Walro, J., Copray, S., Tessarollo, L., and Jaenisch, R. (1998). Neurotrophin-3 and trkC in muscle are non-essential for the development of mouse muscle spindles. Neuroreport *9*, 905–909.

Kuno, M., and Llinas, R. (1970). Alterations of synaptic action in chromatolyzed motoneurones of the cat. J. Physiol. (Lond.) *210*, 823–838.

Lance-Jones, C. (1979). The morphogenesis of the thigh of the mouse with special reference to tetrapod muscle homologies. J. Morphol. *162*, 275–310.

Landgraf, M., Roy, S., Prokop, A., VijayRaghavan, K., and Bate, M. (1999). Even-skipped determines the dorsal growth of motor axons in Drosophila. Neuron *22*, 43–52.

Lichtman, J.W., and Frank, E. (1984). Physiological evidence for specificity of synaptic connections between individual sensory and motor neurons in the brachial spinal cord of the bullfrog. J. Neurosci. *4*, 1745–1753.

Lin, J.H., Saito, T., Anderson, D.J., Lance-Jones, C., Jessell, T.M., and Arber, S. (1998). Functionally related motor neuron pool and muscle sensory afferent subtypes defined by coordinate *ETS* gene expression. Cell *95*, 393–407.

Lumsden, A., and Krumlauf, R. (1996). Patterning the vertebrate neuraxis. Science *274*, 1109–1115.

Ma, Q., Fode, C., Guillemot, F., and Anderson, D.J. (1999). Neurogenin1 and neurogenin2 control two distinct waves of neurogenesis in developing dorsal root ganglia. Genes Dev. *13*, 1717–1728.

McHanwell, S., and Biscoe, T.J. (1981). The localization of motoneurons supplying the hindlimb muscles of the mouse. Philos. Trans. R. Soc. Lond. B. Biol. Sci. *293*, 477–508.

Mears, S.C., and Frank, E. (1997). Formation of specific monosynaptic connections between muscle spindle afferents and motoneurons in the mouse. J. Neurosci. *17*, 3128–3135.

Miller, D.M., and Niemeyer, C.J. (1995). Expression of the unc-4 homeoprotein in Caenorhabditis elegans motor neurons specifies presynaptic input. Development *121*, 2877–2886.

Mo, Y., Vaessen, B., Johnston, K., and Marmorstein, R. (1998). Structures of SAP-1 bound to DNA targets from the E74 and c-fos promoters: insights into DNA sequence discrimination by Ets proteins. Mol. Cell *2*, 201–212.

Mu, X., Silos-Santiago, I., Carroll, S.L., and Snider, W.D. (1993). Neurotrophin receptor genes are expressed in distinct patterns in developing dorsal root ganglia. J. Neurosci. *13*, 4029–4041.

O'Donovan, K.J., Wilkens, E.P., and Baraban, J.M. (1998). Sequential expression of Egr-1 and Egr-3 in hippocampal granule cells following electroconvulsive stimulation. J. Neurochem. *70*, 1241–1248.

Ozaki, S., and Snider, W.D. (1997). Initial trajectories of sensory axons towards laminar targets in the developing mouse spinal cord. J. Comp. Neurol. *380*, 215–229.

Rivero-Melian, C. (1996). Organization of hindlimb nerve projections to the rat spinal cord: a choleragenoid horseradish peroxidase study. J. Comp. Neurol. *364*, 651–663.

Sanes, J.R., and Yamagata, M. (1999). Formation of lamina-specific synaptic connections. Curr. Opin. Neurobiol. *9*, 79–87.

Saueressig, H., Burrill, J., and Goulding, M. (1999). Engrailed-1 and netrin-1 regulate axon pathfinding by association interneurons that project to motor neurons. Development *126*, 4201–4212.

Schaeren-Wiemers, N., and Gerfin-Moser, A. (1993). A single protocol to detect transcripts of various types and expression levels in neural tissue and cultured cells: in situ hybridization using digoxigenin-labelled cRNA probes. Histochemistry *100*, 431–440.

Tanabe, Y., and Jessell, T.M. (1996). Diversity and pattern in the developing spinal cord. Science *274*, 1115–1123.

Tessier-Lavigne, M., and Goodman, C. (1996). The molecular biology of axon guidance. Science *274*, 1123–1133.

Thor, S., Andersson, S.G., Tomlinson, A., and Thomas, J.B. (1999). A LIM-homeodomain combinatorial code for motor-neuron pathway selection. Nature *397*, 76–80.

Tourtellotte, W.G., and Milbrandt, J. (1998). Sensory ataxia and muscle spindle agenesis in mice lacking the transcription factor Egr3. Nat. Genet. *20*, 87–91.

Wasylyk, B., Hagman, J., and Gutierrez-Hartmann, A. (1998). Ets

transcription factors: nuclear effectors of the Ras-MAP-kinase signaling pathway. Trends Biochem. Sci. *270*, 213–216.

Watt, D.G., Stauffer, E.K., Taylor, A., Reinking, R.M., and Stuart, D.G. (1976). Analysis of muscle receptor connections by spike-triggered averaging. 1. Spindle primary and tendon organ afferents. J. Neurophysiol. *39*, 1375–1392.

Weimann, J.M., Zhang, Y.A., Levin, M.E., Devine, W.P., Brulet, P., and McConnell, S.K. (1999). Cortical neurons require Otx1 for the refinement of exuberant axonal projections to subcortical targets. Neuron *24*, 819–831.

Zelena, J. (1994). Nerves and mechanoreceptors—the role of innervation in the development and maintenance of mammalian mechanoreceptors (New York: Chapman and Hall), pp. 1–137.